



# A comparative study of MR extracellular volume fraction measurement and two-dimensional shear-wave elastography in assessment of liver fibrosis with chronic hepatitis B

Kaipu Jin<sup>1</sup> · Heqing Wang<sup>1</sup> · Mengsu Zeng<sup>1</sup> · Shengxiang Rao<sup>1</sup> · Lixia Yan<sup>2</sup> · Yuan Ji<sup>3</sup> · Caixia Fu<sup>4</sup> · Ruofan Sheng<sup>1</sup>

Published online: 7 December 2018

© Springer Science+Business Media, LLC, part of Springer Nature 2018

## Abstract

**Objective** To evaluate the value of MR liver extracellular volume (ECV<sub>liver</sub>) in assessment of liver fibrosis with chronic hepatitis B (CHB), and to compare its performance with two-dimensional (2D) shear-wave elastography (SWE).

**Materials and methods** A total of 68 CHB patients who were histologically diagnosed as fibrosis stages F0 to F4 were retrospectively analyzed. All patients underwent gadopentetate dimeglumine-enhanced T1-mapping and 2D SWE. ECV<sub>liver</sub> and liver stiffness were measured and compared between fibrosis subgroups; their correlations with histologic findings were evaluated using Spearman correlation test and multiple regression analysis. Diagnostic performance in evaluating liver fibrosis stages was assessed and compared using receiver-operating characteristic analysis.

**Results** Both ECV<sub>liver</sub> and liver stiffness increased as the fibrosis score increased ( $F = 17.08$  to  $10.99$ ,  $P < 0.001$ ). ECV<sub>liver</sub> displayed a strong correlation with fibrosis stage ( $r = 0.740$ ,  $P < 0.001$ ), and liver stiffness displayed a moderate correlation ( $r = 0.651$ ,  $P < 0.001$ ); multivariate analysis revealed that only ECV<sub>liver</sub> was independently correlated with fibrosis stage ( $P < 0.001$ ). Univariate analyses showed significant correlations of ECV<sub>liver</sub> with fibrosis stage, inflammatory activity, and platelet count; among all, the fibrosis stage had the highest correlation coefficient and was the only independent factor ( $P < 0.001$ ). Overall, ECV<sub>liver</sub> had no significant different performance compared with 2D SWE for the identification of both fibrosis stage  $s \geq F2$  and  $F4$  ( $P = 0.868$  and  $0.171$ ).

**Conclusion** MR ECV<sub>liver</sub> plays a promising role in the prediction of liver fibrosis for patients with CHB, comparable to 2D SWE.

**Keywords** Liver fibrosis · Extracellular space · Magnetic resonance imaging · Sonoelastography · Chronic hepatitis B · Cirrhosis

## Introduction

Chronic hepatitis B (CHB) infected approximately 240 million patients worldwide and has a high prevalence in China [1]. Liver fibrosis is a key determinant in the natural history of CHB, and untreated fibrosis is likely to progress to cirrhosis with its consequences of portal hypertension, liver failure, and hepatocellular carcinoma [2, 3]. The process of fibrosis is dynamic and a regression of fibrosis is possible in CHB patients [4]. Thus, accurate assessment of liver fibrosis is important to determine prognosis, guide therapeutic strategies, and potential for reversibility. For many years, liver biopsy has been considered the reference standard in liver fibrosis assessment; however, as an

✉ Ruofan Sheng  
ruofansheng@163.com

<sup>1</sup> Department of Radiology, Zhongshan Hospital, Fudan University, Shanghai Institute of Medical Imaging, No. 180 Fenglin Road, Xuhui District, Shanghai 200032, People's Republic of China

<sup>2</sup> Department of Ultrasound, Zhongshan Hospital, Fudan University, Shanghai 200032, People's Republic of China

<sup>3</sup> Department of Pathology, Zhongshan Hospital, Fudan University, Shanghai 200032, People's Republic of China

<sup>4</sup> Siemens Healthcare, Shanghai 200000, People's Republic of China

invasive procedure, biopsy is associated with several risks and limitations [5].

Therefore, noninvasive methods for liver fibrosis assessment have become an intense field of research, including ultrasonography (US) and magnetic resonance imaging (MRI). The use of US elastography is agreed upon in the evaluation of liver stiffness [3], and two-dimensional (2D) shear-wave elastography (SWE) has been proved to have high diagnostic performance for liver fibrosis staging [6, 7]. While liver stiffness measurements in US elastography may be affected by pathological conditions including inflammation, hepatic vascular congestion, and cholestasis; and there is substantial overlap especially between intermediate fibrosis stages [3].

Equilibrium imaging is a technique that uses widely used extracellular contrast agents to evaluate the fractional extracellular volume (ECV) that is expanded in fibrosis and other deposition processes [8]. On equilibrium phase after contrast administration, the concentration of contrast agent within the intravascular compartment is approximately equal to that within the extravascular extracellular compartment [8]. T1 value measurements using T1 mapping before and after contrast enable the calculation of ECV, which may represent the amount of interstitial fibrosis, well-established in myocardial fibrosis assessment [9–11]. When the heart is at contrast equilibrium, other organs may also be at equilibrium, this raises the possibility of extending the technique to a wider use [12]. Until now, MR equilibrium imaging has been rarely applied in liver fibrosis assessment [13, 14]. Therefore, we aimed to evaluate the value of liver extracellular volume ( $ECV_{\text{liver}}$ ) measurement of equilibrium MR in assessment of liver fibrosis among patients with CHB, and to compare its performance with 2D SWE.

## Materials and methods

### Patients

Our institutional review board committee approved this retrospective study, and informed consent was waived. Between April 2017 and December 2017, 233 consecutive adult patients who underwent hepatectomy in the liver surgery department of our institute were recruited. The inclusion criteria were (1) presence of chronic hepatitis B infection (serology test positive for HBV surface antigen) for more than 6 months; (2) availability of liver histologic assessment after surgery; (3) availability of both preoperative gadopentetate dimeglumine-enhanced T1-mapping and 2D SWE. Exclusion criteria were (1) previous history of oncologic treatment or liver resection; (2) diffusive infiltrative or numerous multinodular lesions that hampered

parenchymal evaluation; (3) difficulty to measure T1 mapping values because of poor image quality; (4) failure of 2D SWE; (5) time interval between MR scan/2D SWE and surgery more than 2 weeks; (6) time interval between MR scan and 2D SWE more than 1 week (Fig. 1).

### MRI acquisition

MRI was performed using a 1.5T scanner (Magnetom Aera, Siemens, Erlangen, Germany). Precontrast and equilibrium-phase transverse T1 mapping was conducted using 3D gradient echo sequence with volumetric interpolated breath-hold examination (VIBE), with the following parameters: TE = 1.93 ms, TR = 4.36 ms, slice thickness = 3.5 mm, interslice gap = 0.7 mm, matrix =  $162 \times 288$ , FOV =  $285 \times 380$  mm. Equilibrium-phase T1 mapping was performed 15 min after injection of gadopentetate dimeglumine (Magnevist; Bayer Healthcare, Berlin, Germany) according to existing literatures [13, 14]. Contrast was injected at a dose of 0.1 mmol/kg and rate of 2 mL/s, followed by a 20 mL saline flush using a power injector (Spectris; Medrad, Pittsburgh, PA). Quantitative T1 maps were automatically reconstructed using the MapIt processing tool (MapIt software, Siemens, Erlangen, Germany) after data acquisition.

### MR image analysis

All images were evaluated using a picture archiving and communication system (PACS; Pathspeed, GE Medical Systems Integrated Imaging Solutions, Prospect, IL, USA). Images were measured by two radiologists (K.P.J. and H.Q.W. with 4 and 15 years of abdominal MRI experience), who were blinded to both clinical and histopathological information; measurements from the senior radiologist were used for final analyses. Two individual regions of interest (ROIs) with a fixed size of  $300 \text{ mm}^2$  were drawn on the right posterior lobe and right anterior lobe of liver for the central three continuous sections (six ROIs for each case), on both precontrast- and equilibrium-phase T1-weighted VIBE images, avoiding large vessels, bile ducts, lesions, artifacts, and the border of the liver. The ROIs were then copied to T1 map to measure the T1 relaxation time. Further ROIs were drawn at the same slices as large as possible in the lumen of abdominal aorta (mean area,  $134.8 \text{ mm}^2$  and  $151.1 \text{ mm}^2$  for precontrast- and equilibrium-phase images, respectively), avoiding the aortic wall. Average values were used. ROIs were trying to place at the same axial level before and after contrast (Fig. 2).

By using hematocrit measured from the complete blood count and the precontrast and postcontrast T1 relaxation times of liver and aorta, liver ECV fraction was calculated

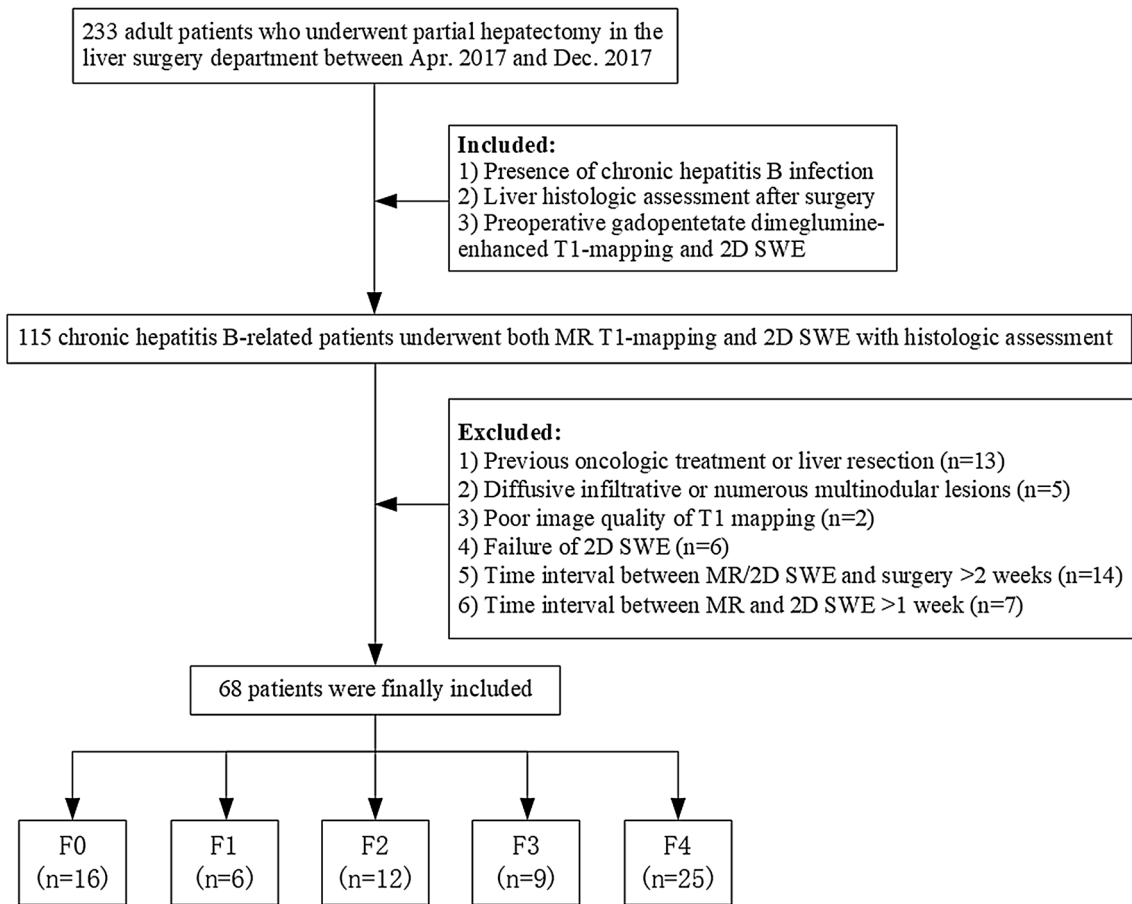


**Fig. 1** Flow chart showing inclusion and exclusion criteria for the study

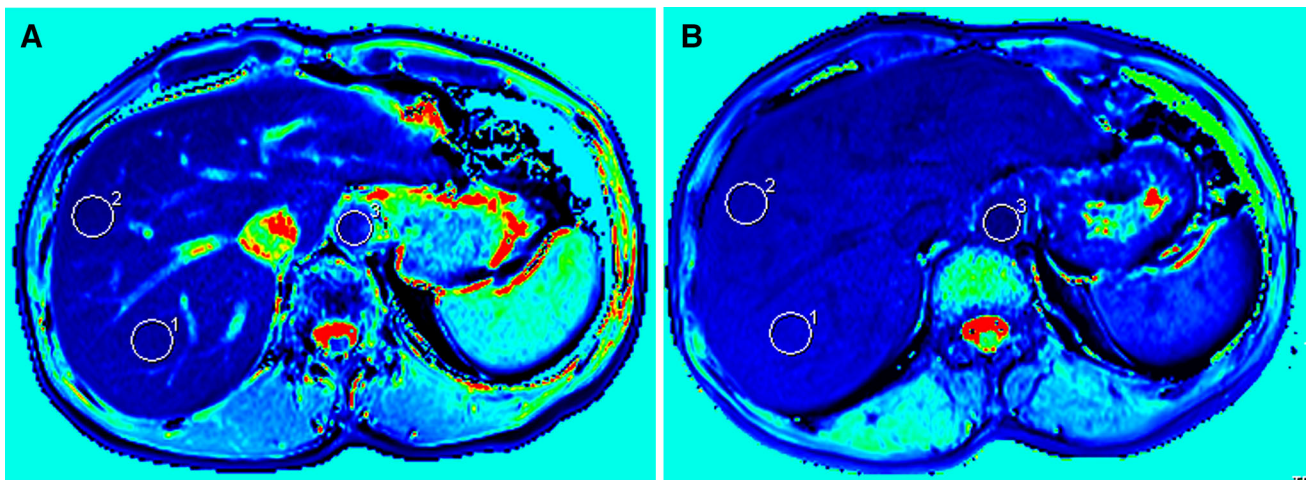


**Fig. 2** A 47-year-old male patient with chronic hepatitis B-related liver fibrosis stage 3. Examples of placement of ROIs in the liver parenchyma and aorta on **a** precontrast- and **b** equilibrium-phase images to measure the T1 relaxation time

as follows [12]:  $ECV_{liver} (\%) = \Delta R1_{liver} / \Delta R1_{aorta} \times (100 - \text{hematocrit})$ , where  $\Delta R1_{liver} = 1/T1_{liver \text{ postcontrast}} - 1/T1_{liver \text{ precontrast}}$  and  $\Delta R1_{aorta} = 1/T1_{aorta \text{ postcontrast}} - 1/T1_{aorta \text{ precontrast}}$ .

## 2D SWE measurements

The 2D SWE measurements were obtained by means of the Aixplorer US imaging system (Supersonic Imagine, Aix-en-Provence, France) and a broadband convex transducer

(SC6–1). All procedures were conducted by three different radiologists in clinical work according to Zhuang et al. [5]. The 2D SWE box ( $40 \times 30 \text{ mm}^2$ ) was placed in the right hepatic lobe. A ROI of approximately 20 mm in diameter was positioned mainly in the center of the box, avoiding large bile ducts, vessels, and the borders of liver and lesions (Fig. 3). Measurements were considered failures when little or no signal was obtained in the 2D SWE box.

### Pathological analysis

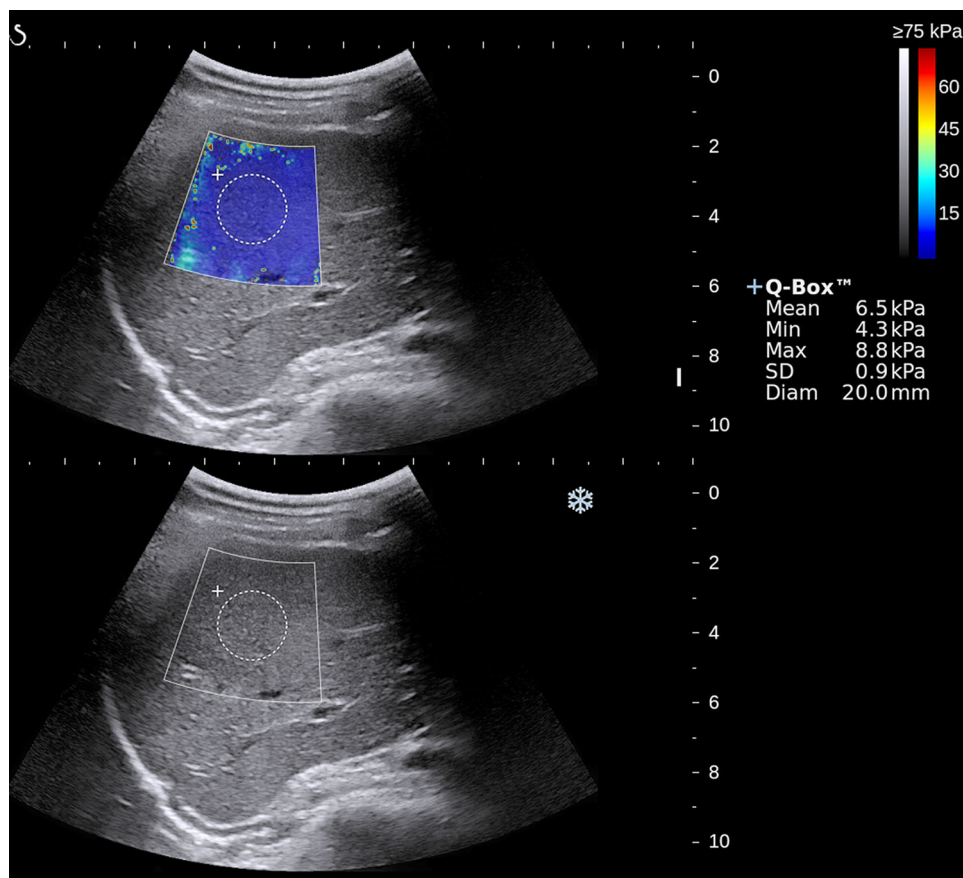
The liver tissues were evaluated for liver fibrosis by a pathologist blinded to the clinical and radiological data (Y.J. with 21 years of experience in liver pathology). The fibrosis stage (“F” grade) and the necroinflammatory activity (“A” grade) were evaluated by the METAVIR scoring system [15]. The degree of fibrosis was defined as follows: F0—no fibrosis; F1—mild fibrosis, portal fibrosis without septa; F2—substantial fibrosis, periportal fibrosis, and few septa; F3—advanced fibrosis, septal fibrosis without cirrhosis; and F4—widespread fibrosis, with cirrhosis. The degree of inflammatory activity was graded as A0—none; A1—mild; A2—moderate; and A3—severe. We defined stages F0–F1 as no or minimal fibrosis with

low likelihood of cirrhosis, F2–F3 as moderate-to-severe fibrosis at risk for progression of the fibrosis [3].

### Statistical analysis

Statistics were summarized as mean  $\pm$  standard deviation or median and interquartile range depending on distributions. The normality was tested using the Kolmogorov–Smirnov test, and the homogeneity of variance was tested using the Levene method. The interobserver agreement of T1 map measurements was assessed by calculating interclass correlation coefficient, and the value greater than 0.75 indicated excellent reliability. Measurements were compared between different fibrosis subgroups using the one-way ANOVA test or Kruskal–Wallis test. Post hoc multiple comparison of individual mean differences was evaluated by using the least significant difference (LSD) or Dunn post hoc test. The correlation between  $\text{ECV}_{\text{liver}}$  and SWE measurement was assessed by Pearson correlation analysis. The correlations between  $\text{ECV}_{\text{liver}}$ , SWE measurements, and the degree of fibrosis were assessed by Spearman correlation analysis and stepwise multiple regression analysis. The strength of Correlation coefficients were classified as follows: 0.0–0.2—very weak to negligible correlation; 0.2–0.4—weak correlation; 0.4–0.7—moderate

**Fig. 3** The 2D shear-wave elastography (top) and gray-scale (bottom) images of the right hepatic lobe in a 28-year-old female patient with chronic hepatitis B



correlation; 0.7–0.9—strong correlation; and 0.9–1.0—very strong correlation [16]. Factors affecting  $ECV_{liver}$  were first analyzed with univariate testing, and those with  $P < 0.05$  were subsequently included in multivariate regression analysis. Diagnostic performance in evaluating liver fibrosis stages was assessed using receiver-operating characteristic (ROC) analysis; areas under the curve (AUCs) with 95% confidence intervals, sensitivity, specificity, and positive and negative predictive values for the classification of fibrosis stage F2 or higher and F4 were calculated. AUCs were compared using the DeLong method [17]. Statistical analyses were performed using SPSS software (version 22.0; Chicago, IL, USA) and Medcalc software (version 15.0; Mariakerke, Belgium). All tests were two-sided, and  $P < 0.05$  was considered statistically significant.

## Results

A total of 68 patients (55 men and 13 women; mean age, 56.81 years; range 24–84 years) were finally included. Baseline clinical characteristics of all patients are presented in Table 1. Histopathologically, 16, 6, 12, 9, and 25

**Table 1** Baseline patient characteristics

Characteristic	
Sex <sup>a</sup> male/female	55 (80.9)/13 (19.1)
Age <sup>b</sup> (years)	58.0 (52.5, 63.0)
Men	58.0 (52.0, 62.0)
Women	61.0 (50.0, 64.5)
Alanine transaminase <sup>b</sup> (U/L)	26.0 (18.0, 37.5)
Aspartate transaminase <sup>b</sup> (U/L)	25.0 (21.0, 40.8)
Total bilirubin <sup>c</sup> ( $\mu\text{mol/L}$ )	14.0 $\pm$ 6.7
Albumin <sup>c</sup> (g/L)	44.2 $\pm$ 4.4
$\gamma$ -glutamyl transferase <sup>b</sup> (U/L)	42.0 (26.3, 92.0)
Platelet count <sup>c</sup> ( $\times 10^9/L$ )	168.7 $\pm$ 65.1
International normalized ratio <sup>b</sup>	1.03 (0.97, 1.07)
Fibrosis stage <sup>b</sup>	
F0	16 (23.53)
F1	6 (8.82)
F2	12 (17.65)
F3	9 (13.24)
F4	25 (36.76)
Focal liver lesions <sup>a</sup>	
Malignant	63 (92.65)
Benign	5 (7.35)

<sup>a</sup>Data are numbers of patients, with percentages in parentheses

<sup>b</sup>Data are medians, with interquartile ranges in parentheses

<sup>c</sup>Data are mean  $\pm$  standard deviation

patients were diagnosed as fibrosis stage F0 to F4, respectively.

## Relationship between $ECV_{liver}$ , 2D SWE measurements, and fibrosis stages

Interobserver agreement showed an excellent interclass correlation coefficient of 0.900 (95% confidence interval: 0.842, 0.938) for  $ECV_{liver}$ .

The  $ECV_{liver}$  and 2D SWE measurements for different fibrosis stages are shown in Table 2. Both  $ECV_{liver}$  and liver stiffness increased as the fibrosis score increased ( $F = 17.08$  to  $10.99$ ,  $P < 0.001$ ), although some overlaps existed among fibrosis stages (Fig. 4).  $ECV_{liver}$  and liver stiffness showed moderate correlation with each other ( $r = 0.497$ ,  $P < 0.0001$ ).

$ECV_{liver}$  showed a strong correlation with fibrosis stage ( $r = 0.740$ ,  $P < 0.001$ ), and liver stiffness showed a moderate correlation with fibrosis stage ( $r = 0.651$ ,  $P < 0.001$ ). Multivariate analysis revealed that only  $ECV_{liver}$  was independently correlated with fibrosis ( $P < 0.001$ ).

## Factors correlating with $ECV_{liver}$

Univariate analyses showed significant correlations of  $ECV_{liver}$  with fibrosis stages ( $r = 0.740$ ), inflammatory activity ( $r = 0.443$ ), and platelet count ( $r = -0.395$ ). Among all the related factors, the fibrosis stage had the highest correlation coefficient and was the only independent factor ( $P < 0.001$ ) (Table 3).

## Diagnostic performance of $ECV_{liver}$ and 2D SWE measurements in fibrosis staging

Diagnostic characteristics of  $ECV_{liver}$  and 2D SWE for prediction of various fibrosis stages are shown in Table 4 and Fig. 5. As for  $ECV_{liver}$ , an AUC of 0.850 with a high specificity of 95.45% was achieved in the diagnosis of moderate to severe fibrosis ( $\geq F2$ ); the AUC was 0.899 with sensitivity and specificity of 84.0% and 83.72%, respectively, in the diagnosis of cirrhosis (F4). Overall,  $ECV_{liver}$  had no significant different performance comparing to 2D SWE for the identification of both fibrosis stage  $\geq F2$  and F4 ( $P = 0.868$  and  $0.171$ ).

## Discussion

With the development and progression of liver fibrosis, extracellular matrix deposits increase and extracellular space are expanded compared with the normal surrounding liver parenchyma [18]. Studies have demonstrated that equilibrium CT imaging can quantitate diffuse liver fibrosis

**Table 2** Statistics of  $ECV_{liver}$  and 2D SWE with the correlation coefficients according to fibrosis stages

	F0	F1	F2	F3	F4	<i>r</i>	<i>P</i>
$ECV_{liver}$	20.26 ± 4.91	23.40 ± 4.56	23.99 ± 3.30	28.32 ± 5.52	32.93 ± 5.91	0.740	< 0.001
2D SWE (kPa)	6.91 ± 2.50	8.78 ± 2.65	10.16 ± 2.55	12.36 ± 4.69	13.92 ± 4.04	0.651	< 0.001

Data are mean ± standard deviation

$ECV_{liver}$  liver fractional extracellular volume, 2D SWE two-dimensional shear-wave elastography

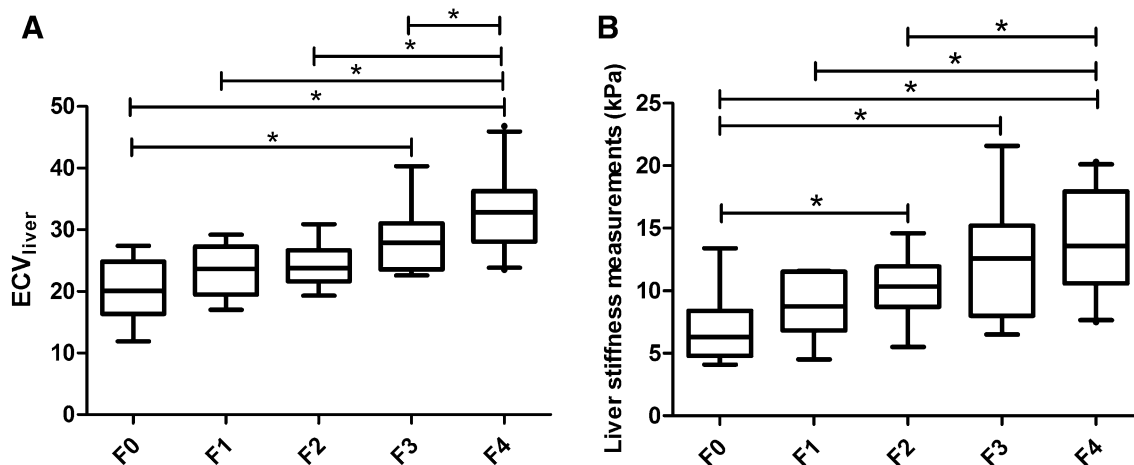


**Fig. 4** Box-and-whisker plots showing median and ranges for **a** liver extracellular volume ( $ECV_{liver}$ ) and **b** liver stiffness of 2D shear-wave elastography (SWE) at different stages of liver fibrosis (\*represents  $P < 0.05$  in pairwise comparisons)

**Table 3** Factors correlating with  $ECV_{liver}$ 

	Univariate correlation test		Multiple regression analysis	
	<i>r</i>	<i>P</i>	$\beta$	<i>P</i>
Fibrosis stage	0.740	< 0.001	0.707	< 0.001
Inflammatory activity	0.443	< 0.001	- 0.033	0.781
Alanine transaminase	0.041	0.739		
Aspartate transaminase	- 0.068	0.581		
Total bilirubin	0.116	0.346		
Albumin	- 0.213	0.082		
$\gamma$ -glutamyl transferase	0.042	0.732		
Platelet count	- 0.395	0.001	- 0.009	0.927
International normalized ratio	0.239	0.052		
Age	0.061	0.622		
Sex	- 0.091	0.458		

$ECV_{liver}$  liver fractional extracellular volume

in both animals and patients [8, 18, 19]; while a few referred to MR equilibrium imaging, with either limited number of patients or no histopathological Ref. [13, 14]. Our study confirmed previous results in a considerable number of CHB-related patients with exact pathology, and indicated a strong correlation between  $ECV_{liver}$  and liver fibrosis stage. Meanwhile, there are several other processes that may affect ECV and confound fibrosis measurement:

for example, edema from inflammation may expand  $ECV_{liver}$  [8]. Our results indicated that fibrosis stage was the only factor independently predicted by  $ECV_{liver}$ , compared to other potential confounders including inflammation activity. Thus, we considered  $ECV_{liver}$  as a reliable technique in assessing liver fibrosis for patients with CHB.

Cirrhosis is strongly associated with liver-related morbidity and mortality, and is the most important question in

**Table 4** Diagnostic performance of  $ECV_{liver}$  and 2D SWE for evaluating fibrosis stages

	AUC (95% CI)	Cutoff	Sen (%)	Spe (%)	PPV (%)	NPV (%)
$ECV_{liver}$						
$\geq F2$	0.850 (0.742,0.925)	> 27.4	58.70	95.45	96.4	52.5
F4	0.899 (0.801,0.959)	> 27.42	84.00	83.72	75.0	90.0
2D SWE						
$\geq F2$	0.860 (0.754,0.932)	> 10	71.74	86.36	91.7	59.4
F4	0.811 (0.697,0.896)	> 11.6	68.00	79.07	65.4	81.0

$ECV_{liver}$  liver fractional extracellular volume, 2D SWE two-dimensional shear-wave elastography, AUC area under the curve, CI confidence interval, Sen sensitivity, Spe specificity, PPV positive predictive value, NPV negative predictive value

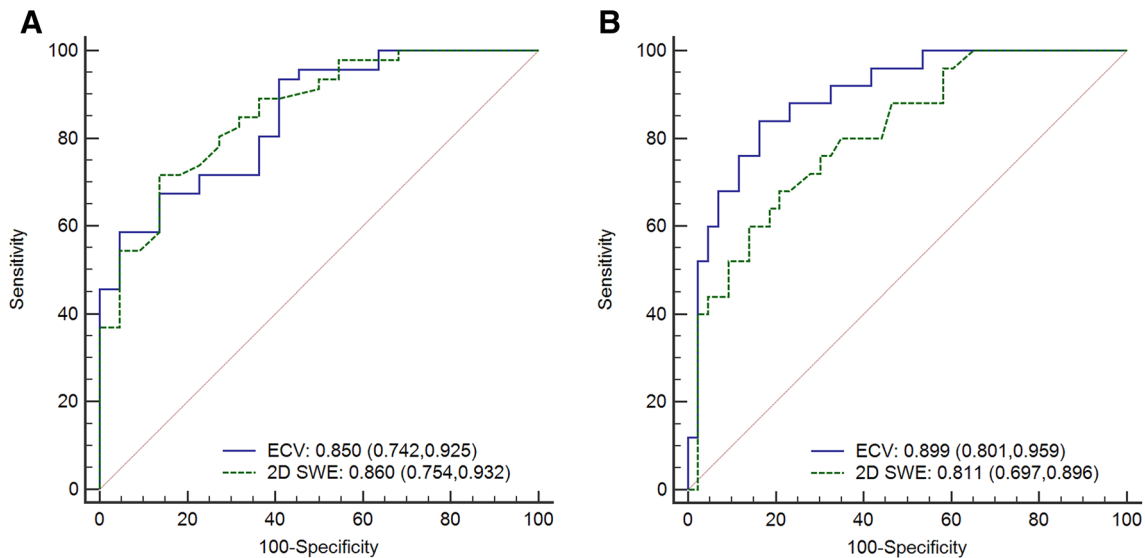


**Fig. 5** Receiver-operating characteristic curves for the identification of liver fibrosis stages **a**  $F \geq 2$ , and **b** F4 using liver extracellular volume ( $ECV_{liver}$ ) and 2D shear-wave elastography (SWE). Numbers indicate areas under the curve with 95% confidence intervals in parentheses

patients with chronic liver disease. Although some findings, including low platelet count and a nodular liver surface on images, can indicate the presence of cirrhosis, these findings are often absent in compensated cirrhosis [3]. Our results showed high diagnostic performance of  $ECV_{liver}$  in determining cirrhosis with an AUC value of 0.899 and satisfied sensitivity and specificity of 84.0% and 83.72%, respectively. However, the diagnostic efficacy of  $ECV_{liver}$  in identification between no and minimal fibrosis and moderate to severe fibrosis was not that satisfactory, showing a fair AUC value and lack of high sensitivity. The possible reason may be that, the initial step of fibrogenesis is the activation and proliferation of hepatic stellate cells, and a large number of them has been activated before extensive deposition of extracellular matrix [20]. In spite of the unsatisfied sensitivity, a high specificity greater than 90% was achieved in predicting fibrosis stage F2 or higher.

$ECV_{liver}$  was moderately correlated with liver stiffness. Comparing to 2D SWE,  $ECV_{liver}$  showed a stronger correlation with fibrosis stages, and a better diagnostic

performance in identification of cirrhosis although no statistical significance existed. Furthermore,  $ECV_{liver}$  estimation is not affected by pathological conditions including cellular edema and cholestasis, which are drawbacks of elastographic techniques [13]. It is a scanning protocol independent of field strength with no need of additional expensive equipment and experienced investigators [13], and has the potential to sample the entire liver volume and detect regional variation of fibrosis based on parenchymal heterogeneity [14]. Considering the advantages,  $ECV_{liver}$  may be a comparable or even superior tool in comparison to 2D SWE, which can be easily implemented into routine clinical liver MRI examinations in CHB patients.

This study had several limitations. First, because of the retrospective nature, 2D SWE examinations were conducted by three different radiologists in clinical work, although a uniform SWE operation standard was set, inconsistency among observers was inevitable; this also partially explains the relatively inferior diagnostic performance of SWE in our study. Further prospectively study is

needed in future work. Second, ROI of the left lobe was not chosen for T1 mapping measurements, as ROI of liver stiffness measurements in 2D SWE was placed in the right lobe, and the stability of T1 values may be influenced by the relatively significant artifact in the left hepatic lobe. Third, we focused on the comparison analyses with SWE in this study, and did not compare ECV<sub>liver</sub> with other MR imaging methods including the well-established technique MR elastography. But the relative high cost, need for additional hardware and software, and non-widespread availability of MR elastography limit its applicability [21]; while MR-ECV has its own advantages as it is a scanning protocol based on simple calculations which needs no additional equipment, and may be easily implemented to routine clinical liver MR examinations.

In conclusion, MR ECV<sub>liver</sub> plays a promising role in the prediction of liver fibrosis for patients with CHB, comparable with 2D SWE.

**Funding** This work was supported by the National Natural Science Foundation for Young Scientists of China [grant number 81601488]; the Shanghai Sailing Program [grant number 16YF1410600]; and the National Natural Science Foundation of China [grant number 81571661].

## References

- Lok AS, McMahon BJ, Brown RS, Jr., Wong JB, Ahmed AT, Farah W, Almasri J, Alahdab F, Benkhadra K, Mouchli MA, Singh S, Mohamed EA, Abu Dabrh AM, Prokop LJ, Wang Z, Murad MH, Mohammed K (2016) Antiviral therapy for chronic hepatitis B viral infection in adults: A systematic review and meta-analysis. *Hepatology* 63 (1):284–306. <https://doi.org/10.1002/hep.28280>
- Polasek M, Fuchs BC, Uppal R, Schuehle DT, Alford JK, Loving GS, Yamada S, Wei L, Lauwers GY, Guimaraes AR, Tanabe KK, Caravan P (2012) Molecular MR imaging of liver fibrosis: A feasibility study using rat and mouse models. *J Hepatol* 57 (3):549–555. <https://doi.org/10.1016/j.jhep.2012.04.035>
- Barr RG, Ferraioli G, Palmeri ML, Goodman ZD, Garcia-Tsao G, Rubin J, Garra B, Myers RP, Wilson SR, Rubens D, Levine D (2015) Elastography Assessment of Liver Fibrosis: Society of Radiologists in Ultrasound Consensus Conference Statement. *Radiology* 276 (3):845–861. <https://doi.org/10.1148/radiol.2015150619>
- Marcellin P, Gane E, Buti M, Afdhal N, Sievert W, Jacobson IM, Washington MK, Germanidis G, Flaherty JF, Aguilar Schall R, Bornstein JD, Kitrinis KM, Subramanian GM, McHutchison JG, Heathcote EJ (2013) Regression of cirrhosis during treatment with tenofovir disoproxil fumarate for chronic hepatitis B: a 5-year open-label follow-up study. *Lancet* 381 (9865):468–475. [https://doi.org/10.1016/s0140-6736\(12\)61425-1](https://doi.org/10.1016/s0140-6736(12)61425-1)
- Yoon JH, Lee JM, Baek JH, Shin C-i, Kiefer B, Han JK, Choi B-I (2014) Evaluation of Hepatic Fibrosis Using Intravoxel Incoherent Motion in Diffusion-Weighted Liver MRI. *J Comput Assist Tomogr* 38 (1):110–116. <https://doi.org/10.1097/RCT.0b013e3182a589be>
- Zhuang Y, Ding H, Zhang Y, Sun HC, Xu C, Wang WP (2017) Two-dimensional Shear-Wave Elastography Performance in the Noninvasive Evaluation of Liver Fibrosis in Patients with Chronic Hepatitis B: Comparison with Serum Fibrosis Indexes. *Radiology* 283 (3):872–881. <https://doi.org/10.1148/radiol.2016160131>
- Barr RG (2017) Shear wave liver elastography. *Abdom Radiol (NY)*. <https://doi.org/10.1007/s00261-017-1375-1>
- Bandula S, Punwani S, Rosenberg WM, Jalan R, Hall AR, Dhillon A, Moon JC, Taylor SA (2015) Equilibrium Contrast-enhanced CT Imaging to Evaluate Hepatic Fibrosis: Initial Validation by Comparison with Histopathologic Analysis. *Radiology* 275 (1):136–143. <https://doi.org/10.1148/radiol.14141435>
- Everett RJ, Stirrat CG, Semple SIR, Newby DE, Dweck MR, Mirsadraee S (2016) Assessment of myocardial fibrosis with T1 mapping MRI. *Clin Radiol* 71 (8):768–778. <https://doi.org/10.1016/j.crad.2016.02.013>
- Brouwer WP, Baars EN, Germans T, de Boer K, Beek AM, van der Velden J, van Rossum AC, Hofman MBM (2014) In-vivo T1 cardiovascular magnetic resonance study of diffuse myocardial fibrosis in hypertrophic cardiomyopathy. *J Cardiovasc Magn Reson*. <https://doi.org/10.1186/1532-429x-16-28>
- Schelbert EB, Messroghli DR (2016) State of the Art: Clinical Applications of Cardiac T1 Mapping. *Radiology* 278 (3):658–676. <https://doi.org/10.1148/radiol.2016141802>
- Bandula S, Banyersad SM, Sado D, Flett AS, Punwani S, Taylor SA, Hawkins PN, Moon JC (2013) Measurement of Tissue Interstitial Volume in Healthy Patients and Those with Amyloidosis with Equilibrium Contrast-enhanced MR Imaging. *Radiology* 268 (3):858–864. <https://doi.org/10.1148/radiol.13121889/-/DC1>
- Luetkens JA, Klein S, Traeber F, Schmeel FC, Sprinkart AM, Kuetting DLR, Block W, Hittatiya K, Uschner FE, Schierwagen R, Gieseke J, Schild HH, Trebicka J, Kukuk GM (2017) Quantitative liver MRI including extracellular volume fraction for non-invasive quantification of liver fibrosis: a prospective proof-of-concept study. *Gut*. <https://doi.org/10.1136/gutjnl-2017-314561>
- Wells ML, Moynagh MR, Carter RE, Childs RA, Leitch CE, Fletcher JG, Yeh BM, Venkatesh SK (2017) Correlation of hepatic fractional extracellular space using gadolinium enhanced MRI with liver stiffness using magnetic resonance elastography. *Abdom Radiol (NY)* 42 (1):191–198. <https://doi.org/10.1007/s00261-016-0867-8>
- Goodman ZD (2007) Grading and staging systems for inflammation and fibrosis in chronic liver diseases. *J Hepatol* 47 (4):598–607. <https://doi.org/10.1016/j.jhep.2007.07.006>
- Karlik SJ (2003) Exploring and summarizing radiologic data. *AJR Am J Roentgenol* 180 (1):47–54
- DDelong ER, DeLong DM, Clarkepearson DI (1988) Comparing the areas under two or more correlated receiver operating characteristic curves: a nonparametric approach. *Biometrics* 44 (3):837–845. <https://doi.org/10.2307/2531595>
- Guo SL, Su LN, Zhai YN, Chirume WM, Lei JQ, Zhang H, Yang L, Shen XP, Wen XX, Guo YM (2017) The clinical value of hepatic extracellular volume fraction using routine multiphase contrast-enhanced liver CT for staging liver fibrosis. *Clin Radiol* 72 (3):242–246. <https://doi.org/10.1016/j.crad.2016.10.003>
- Varenika V, Fu Y, Maher JJ, Gao D, Kakar S, Cabarrus MC, Yeh BM (2013) Hepatic Fibrosis: Evaluation with Semiquantitative Contrast-enhanced CT. *Radiology* 266 (1):151–158. <https://doi.org/10.1148/radiol.12112452>
- Moreira RK (2007) Hepatic stellate cells and liver fibrosis. *Arch Pathol Lab Med* 131 (11):1728–1734. [https://doi.org/10.1043/1543-2165\(2007\)131\[1728:hscalf\]2.0.co;2](https://doi.org/10.1043/1543-2165(2007)131[1728:hscalf]2.0.co;2)
- Mathew RP, Venkatesh SK (2018) Imaging of Hepatic Fibrosis. *Curr Gastroenterol Rep* 20 (10):45. <https://doi.org/10.1007/s11894-018-0652-7>